

# Stereomicroscopic features of colitis-associated tumors in mice: Evaluation of pit pattern

RYOSUKE YAMAUCHI<sup>1</sup>, KEN KOMINATO<sup>1</sup>, KEIICHI MITSUYAMA<sup>1,2</sup>, HIDETOSHI TAKEDATSU<sup>1</sup>, SHINICHIRO YOSHIOKA<sup>1</sup>, KOTARO KUWAKI<sup>1</sup>, HIROSHI YAMASAKI<sup>1</sup>, SHUHEI FUKUNAGA<sup>1</sup>, ATSUSHI MORI<sup>1</sup>, JUN AKIBA<sup>3</sup>, OSAMU TSURUTA<sup>1</sup> and TAKUJI TORIMURA<sup>1</sup>

<sup>1</sup>Division of Gastroenterology, Department of Medicine; <sup>2</sup>Inflammatory Bowel Disease Center, Kurume University School of Medicine; <sup>3</sup>Department of Diagnostic Pathology, Kurume University Hospital, Kurume, Fukuoka 830-0011, Japan

Received September 30, 2016; Accepted March 3, 2017

DOI: 10.3892/ol.2017.6645

**Abstract.** Patients with longstanding ulcerative colitis have an increased risk of colorectal cancer. Mouse models for colitis-associated tumors are indispensable for the development of novel strategies for prevention and intervention, as well as an improved understanding of the mechanisms underlying tumor formation. The present study examined whether stereomicroscopic observations with dye-application were able to detect and discriminate tumors in a colitis-associated tumor model in mice. Colonic tumors were induced in C57BL/6 mice by 15 cycles of treatment with dextran sulfate sodium (DSS) in drinking water. The mice were then divided into 4 groups: normal mice fed a control diet, normal mice fed an iron-supplemented diet, 0.7% DSS mice fed an iron diet and 1.5% DSS mice fed an iron diet. The entire colons were characterized with respect to both morphology and histology. The pit pattern architecture was analyzed using stereomicroscopy with dye agents (0.2% indigo carmine or 0.06% crystal violet). The tumor histology was graded as negative, indefinite or positive for dysplasia. The positive category was divided into two subcategories: low-grade dysplasia (LGD) and high-grade dysplasia (HGD). The tumor incidences and multiplicity were significantly higher in mice fed an iron diet and 1.5% DSS compared with in mice fed an iron diet and 0.7% DSS. Compared with LGD, HGD was predominantly located in the distal colon, was larger in size and had a higher incidence of elevated lesions (Is and IIa) and a lower incidence of flat lesions (IIb). In regards to the pit pattern, HGD had a high incidence of V<sub>1</sub> pits and a low incidence of IV, III<sub>L</sub> and II pits. In conclusion, evaluation of the pit pattern using stereomicroscopy with dye-application is useful for detecting

and discriminating neoplastic changes in DSS mice and may further our understanding of the mechanisms that induce tumor formation in patients with ulcerative colitis and the characterization of pharmaceutical responses.

## Introduction

Ulcerative colitis (UC) is a chronic relapsing disorder associated with uncontrolled inflammation within the gastrointestinal tract (1). Patients with longstanding UC have an increased risk of colorectal cancer (2,3). The molecular pathway that induces cancer in UC appears to differ from the well-known 'adenoma-carcinoma sequence', as these types of cancer often develop in flat or mildly elevated lesions and are distributed multifocally within an area of intestinal inflammation, called the 'inflammation-dysplasia-carcinoma sequence' (4-6). Therefore, the timely colonoscopic detection and diagnosis of neoplasia during early phase is crucially important for treatment.

Previously, chromoendoscopy with dye-spraying, which provides a more detailed visualization of the mucosa by enhancing its morphology, was developed to improve upon the accuracy afforded by conventional endoscopy (7-9). The authors of the present study (10,11) and other studies (12-16) have previously demonstrated that this imaging technique facilitates the detection of early-stage neoplastic lesions in UC.

Animal models of colitis-associated tumors for the study of cancer prevention and early detection have been reported (17,18). The oral administration of dextran sulfate sodium (DSS) to mice has been revealed to induce colonic inflammation that is clinically and histologically similar to UC (19). Furthermore, the repeated administration of DSS may induce dysplastic/cancerous lesions via the 'inflammation-dysplasia-carcinoma sequence' (20). If a detailed analysis of focal mucosal lesions is possible with the present model, it may be useful for identifying microscopic lesions, which would result in an improved understanding of the mechanisms underlying tumor formation and the development of novel strategies for prevention and intervention.

The present study induced colitis-associated tumors in mice and subsequently determined whether stereomicroscopic observation with dye-application may be used to detect and discriminate the tumors.

---

*Correspondence to:* Professor Keiichi Mitsuyama, Inflammatory Bowel Disease Center, Kurume University School of Medicine, Asahi-machi 67, Kurume, Fukuoka 830-0011, Japan  
E-mail: ibd@med.kurume-u.ac.jp

**Key words:** colitis, ulcerative colitis, cancer, dysplasia, pit pattern, mouse

## Materials and methods

**Ethical approval.** Prior to the initiation of this study, the experimental protocol was examined and approved by the Animal Research Committee of Kurume University (Kurume, Japan). The present study was undertaken with strict adherence to the recommendations in the Guide for the Care and Use of Laboratory Animals of the National Institute of Health (21) and extra care was taken to avoid animal suffering.

**Mice and treatment.** C57BL/6 7-8-week-old female mice ( $n=67$ ; mean weight, 19.1 g) were purchased from SLC Co., Ltd., Shizuoka, Japan. Mice were housed in standard wire-mesh cages and provided with drinking water with or without 0.7% or 1.5% DSS (molecular weight, 40,000; ICN Biomedicals, Aurora, OH, USA) for 7 days, followed by water without any additives for the next 10 days. The mice were fed a standard basal diet (AIN-76; for its composition, see <http://www.test-diet.com>) or a basal diet enriched 2-fold with iron (final iron concentration, 90 mg/kg) (22,23). These mice were allowed free access to water and rodent chow. When mice exhibited moribund symptoms, including i) lack of responsiveness to manual stimulation, ii) immobility or iii) an inability to eat or drink, they reached the humane endpoints (24). Following 15 treatment cycles, the surviving mice were weighed and sacrificed with carbon dioxide asphyxiation and their colons were investigated morphologically and histologically.

The mice were divided into 4 groups: Normal mice fed a control diet; normal mice fed an iron-supplemented diet; 0.7% DSS mice fed an iron diet; and 1.5% DSS mice fed an iron diet (Fig. 1). The mean weight change after each treatment was 136.9, 137.7, 139.3 and 119.1%, respectively.

**Assessment of colitis.** A clinical score was generated based on a 0-4 rating of the following factors: Change in body weight, stool consistency and intestinal bleeding (25,26). Each variable was allocated equal weight, with the overall clinical activity score ranging from 0-12. These parameters were determined by an investigator who was blinded to the treatment group. Following randomization, a histologic score was assigned by two pathologists who were also group-blinded.

Sections stained with hematoxylin and eosin were histopathologically evaluated for the severity of colitis in a blinded manner, as described previously (27). The histologic score for each segment (cecum, proximal colon, middle colon and distal colon) ranged from 0-9 and represented the sum of the scores for the severity of inflammation, damage/necrosis and regeneration. The total histologic score ranged from 0-12 and consisted of the sum of the score for the distal colon and the score for disease extent.

The severity of colitis was also determined based on the colonic length from the ceco-colonic junction to the anal verge, as this evaluation is an established inflammatory parameter for DSS-induced colitis (19).

**Tumor morphology.** The macroscopic features of the tumors were classified according to size, shape and location. The size of each lesion was determined by determining the largest diameter of the lesion using an ocular micrometer. The shape of each lesion was classified based on the Paris endoscopic

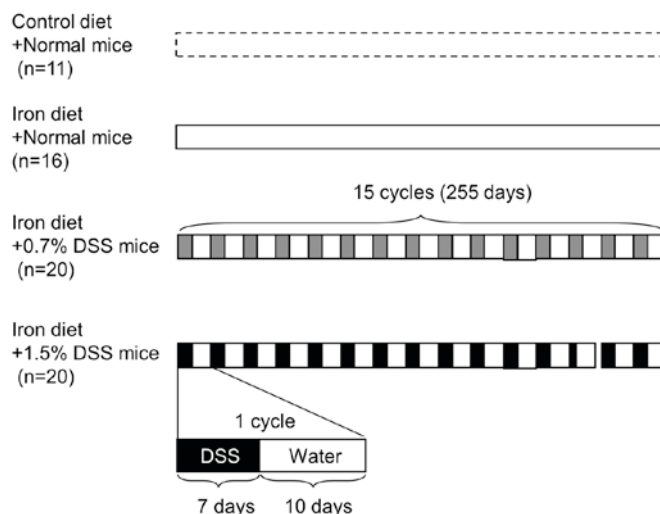


Figure 1. Experimental protocol for chronic DSS-induced colitis in mice. Female mice 7-8 weeks old were provided with water with 0.7 or 1.5% DSS for 7 days, followed by a 10-day period of water without any additives. The mice were fed with a standard basal diet that was enriched 2-fold with iron. Following 15 cycles, the surviving mice were weighed and sacrificed and their colons were histologically and morphologically evaluated. DSS, dextran sulfate sodium.

classification (28) used in human pathology studies of colorectal cancer (Fig. 2).

**Pit pattern diagnosis.** *Ex vivo* observations using Nikon SMZ-1000 stereomicroscope (Nikon Corporation, Tokyo, Japan) were performed after the topical application of 0.06% crystal violet or 0.2% indigo carmine for 30-40 sec at room temperature to enhance mucosal details. Crystal violet stains the circumferential convex portions, but not the grooves, whereas indigo carmine does not stain the colonic mucosa but accumulates inside the grooves, highlighting subtle mucosal irregularities (29).

The pit pattern classification by Kudo *et al* (30,31) divides colorectal lesions into 5 classes (Fig. 3). Only focal mucosal lesions that were distinguished clearly from the surrounding mucosa were classified according to the pit pattern classification, due to inflammatory alterations often displaying mucosal irregularities. Type I pit pattern represents regular round crypts, type II pattern represents stellar or papillary crypts, type III pattern represents small tubular or roundish crypts ( $III_s$ ) or large tubular or roundish crypts ( $III_L$ ), type IV pattern consists of branch- or gyrus-like crypts and type V pattern consists of irregular crypts ( $V_I$ ) or non-structural crypts ( $V_N$ ). For lesions exhibiting multiple pit patterns, the pit pattern of the most atypical area was used.

**Histopathology.** Each specimen was treated with 10% neutral-buffered formalin and sectioned at a 4- $\mu$ m thickness and stained using hematoxylin and eosin (H&E). Two gastrointestinal pathologists who were blinded as to the stereomicroscopic diagnosis examined all the specimens by using a Nikon Optiphot microscope (Nikon Corporation). Based on the classification by Riddell *et al* (32), the tumor histology was categorized as negative, indefinite or positive for dysplasia. The positive category was divided into two subcategories:

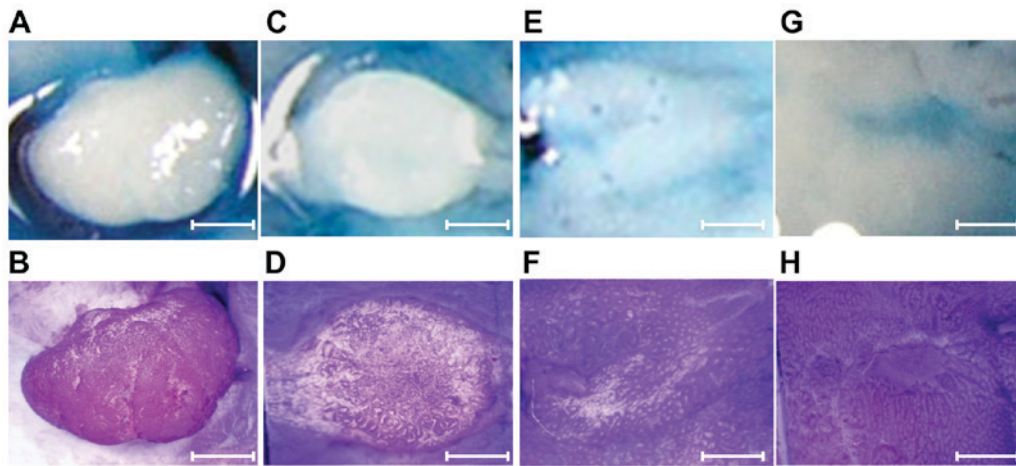


Figure 2. Criteria for the classification of macroscopic appearances. Lesions are classified as (A and B) sessile (type Is), (C and D) elevated (type IIa), (E and F) flat (type IIb) or (G and H) depressed lesions (type IIc). (A, C, E and G) Following topical application of 0.2% indigo carmine and (B, D, F and H) following topical application of 0.06% crystal violet. Scale bar, 1 mm.

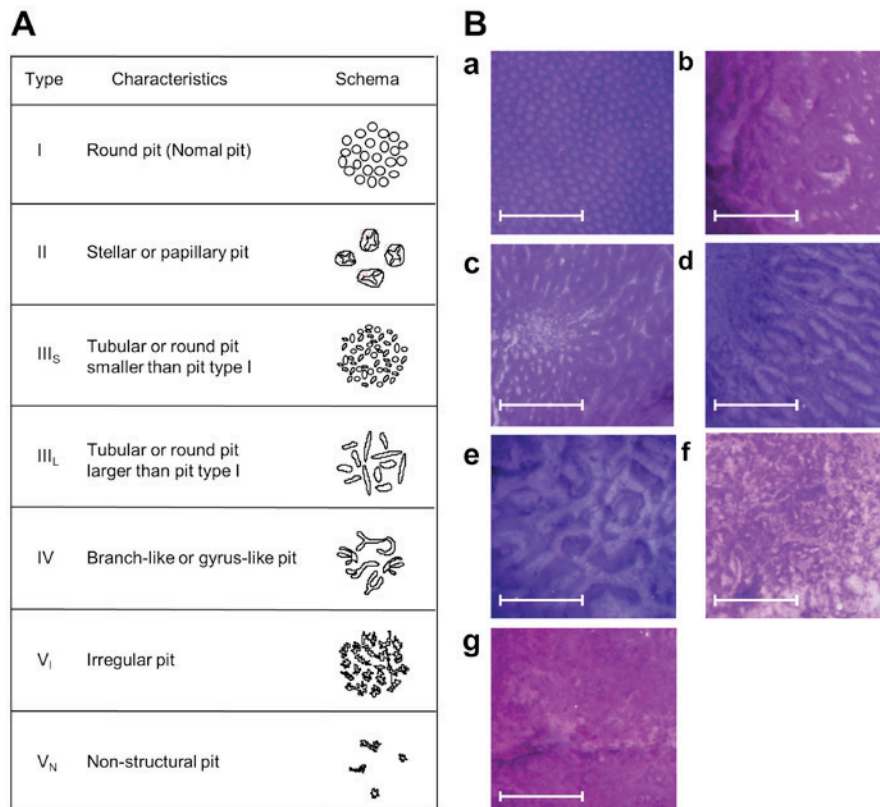


Figure 3. Criteria for the classification of pit patterns according to Kudo *et al* (30). (A) A schematic illustration. The colonic crypt architecture was classified and divided into 5 classes. (B) Representative high-resolution views using stereomicroscopy with 0.06% crystal violet staining. The colonic crypt architecture was classified using high magnification chromoscopy with crystal violet spraying. Representative pictures of each type of lesion are presented. (a) A type I pit pattern consists of regular round crypts, (b) a type II pattern consists of stellar or papillary crypts, (c) a type III pattern consists of small tubular or roundish crypts (III<sub>s</sub>) or (d) large tubular or roundish crypts (III<sub>L</sub>), (e) a type IV pattern consists of branch- or gyrus-like crypts and (f) a type V pattern consists of irregular crypts (V<sub>I</sub>) or (g) non-structural crypts (V<sub>N</sub>). For lesions exhibiting multiple pit patterns, the pit pattern of the most atypical area was adopted. Scale bar, 100  $\mu$ m.

Low-grade dysplasia (LGD) and high-grade dysplasia (HGD; Table I; Fig. 4) (32,33).

**Statistical analysis.** Where the data were normally distributed, a single analysis of variance was used to identify regional differences and the differences between groups was analyzed using the Tukey-Kramer honestly significant difference test

(JMP statistical package version 12; SAS Institute, Cary, NC, USA). Where the data was not normally distributed, the differences were analyzed using the nonparametric Wilcoxon/Kruskal-Wallis test (rank sums). The probability of survival analysis was estimated using the Kaplan-Meier method. The statistical significance of each comparison was determined using the log-rank test. The results are presented

Table I. The histological classification of dysplasia by Riddell *et al* (32).

Negative	Normal mucosa	Inactive colitis	Active colitis
Indefinite	Probably negative (probably inflammatory)	Unknown	Probably positive (probably dysplastic)
Positive	Low-grade dysplasia	High-grade dysplasia	-

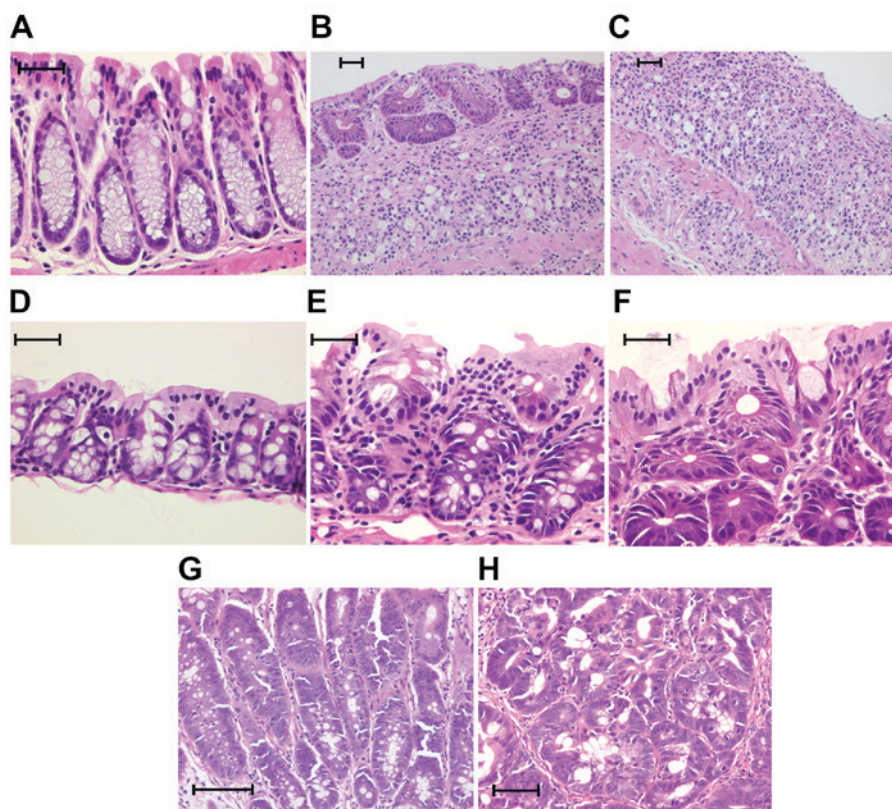


Figure 4. Histological classification of dysplasia by Riddell *et al* (32). Microscopic photographs of representative cases for each category are presented: (A) Normal mucosa; (B) inactive colitis; (C) active colitis; (D) probably negative; (E) unknown; (F) probably positive; (G) low-grade dysplasia; (H) high-grade dysplasia (all stained with hematoxylin and eosin). (A, D-H) Original magnification, x40; scale bar, 50  $\mu$ m; (B and C) original magnification; x10, scale bar, 100  $\mu$ m.

as the mean  $\pm$  standard error.  $P < 0.05$  was considered to indicate a statistically significant difference.

## Results

**Time course for DSS-induced colitis.** Food consumption remained unchanged among the controls and iron-supplemented mice at the end of the experiment (data not shown). Higher disease activity scores were evident in the 1.5% DSS mice fed an iron-enriched diet, compared with the normal mice fed a control diet ( $P < 0.0001$ ), the normal mice fed an iron-enriched diet ( $P < 0.0001$ ) and the 0.7% DSS mice fed an iron diet ( $P = 0.004$ ; Fig. 5A). The 1.5% DSS mice (mean  $\pm$  standard deviation,  $22.8 \pm 3.1$  g; minimum weight, 18.5 g; maximum weight, 27.0 g) had a lower body weight than the control mice ( $26.1 \pm 1.3$  g; minimum weight, 24.0 g; maximum weight, 28.0 g) at the end of the experiment, although the difference was not statistically significant (Fig. 5B). A total of 10 mice from the 1.5% DSS mice fed an iron diet succumbed prior to completion of 15 DSS cycles; these mice exhibited significant weight loss, severe rectal bleeding and diarrhea and extensive ulceration of

the colon. However, no colon tumors were identified, indicating that the probable cause of mortality was not cancer development but severe colonic inflammation (Fig. 5C).

**Colonic damage in DSS-induced colitis.** Colonic damage was assessed according to the colonic length and histologic scores. Drinking water containing DSS resulted in colon injury, as determined according to the colon length; the colon injury was more severe in the 1.5% DSS mice fed an iron-enriched diet compared with in the 0.7% DSS mice fed an iron-enriched diet (Fig. 6). Mice that underwent the repeated administration of DSS exhibited colitis, particularly in the distal colon. Higher pathological scores were demonstrated in the 1.5% DSS mice fed an iron-enriched diet, compared with 0.7% DSS mice fed an iron-enriched diet (Fig. 7). Notably, mild inflammation was revealed in the normal mice fed an iron-enriched diet compared with the normal mice on the control diet ( $P < 0.0001$ ).

**Incidence of dysplasia in DSS-induced colitis.** The results for tumor incidence are presented in Table II. LGD, but not HGD, was observed in one normal mouse fed the iron-enriched

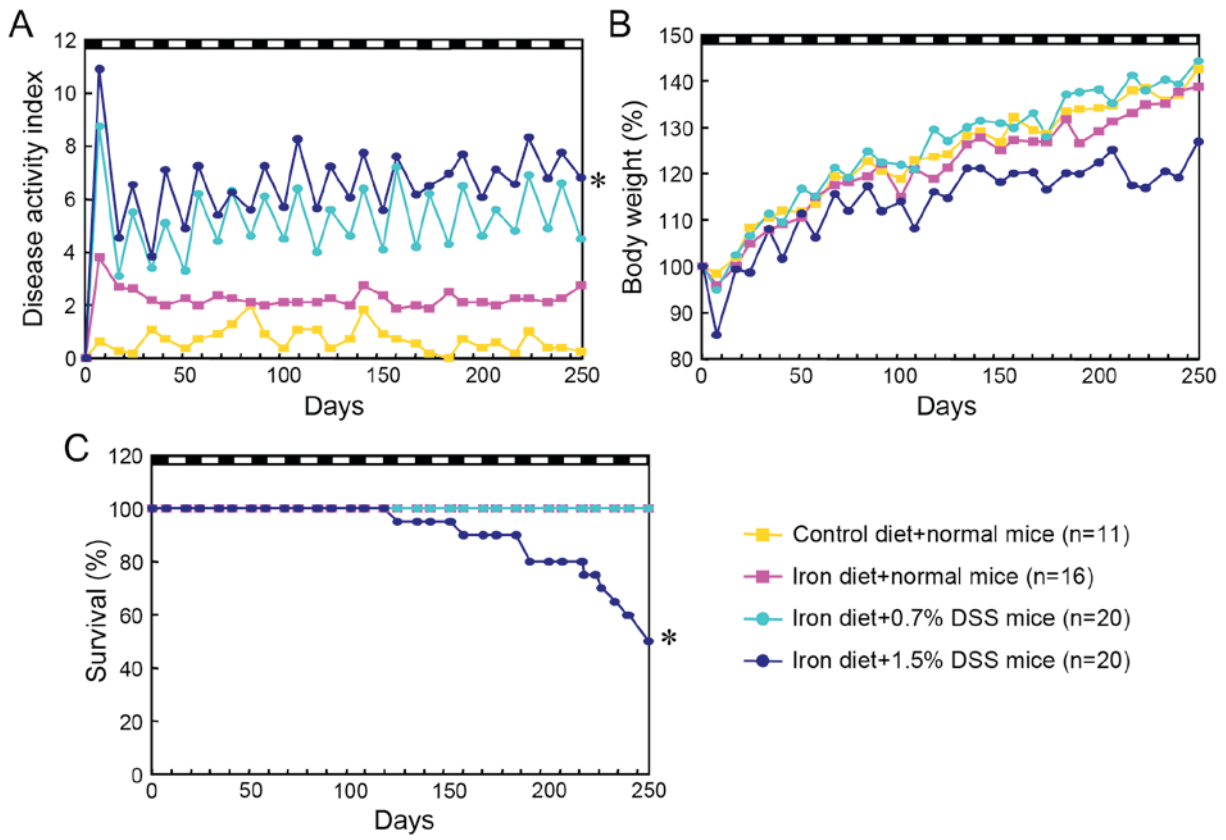


Figure 5. Serial changes in (A) disease activity score, (B) body weight and (C) survival during the course of chronic DSS-induced colitis. \*P<0.0001 vs. in the normal mice fed a control diet at day 250. DSS, dextran sulfate sodium.

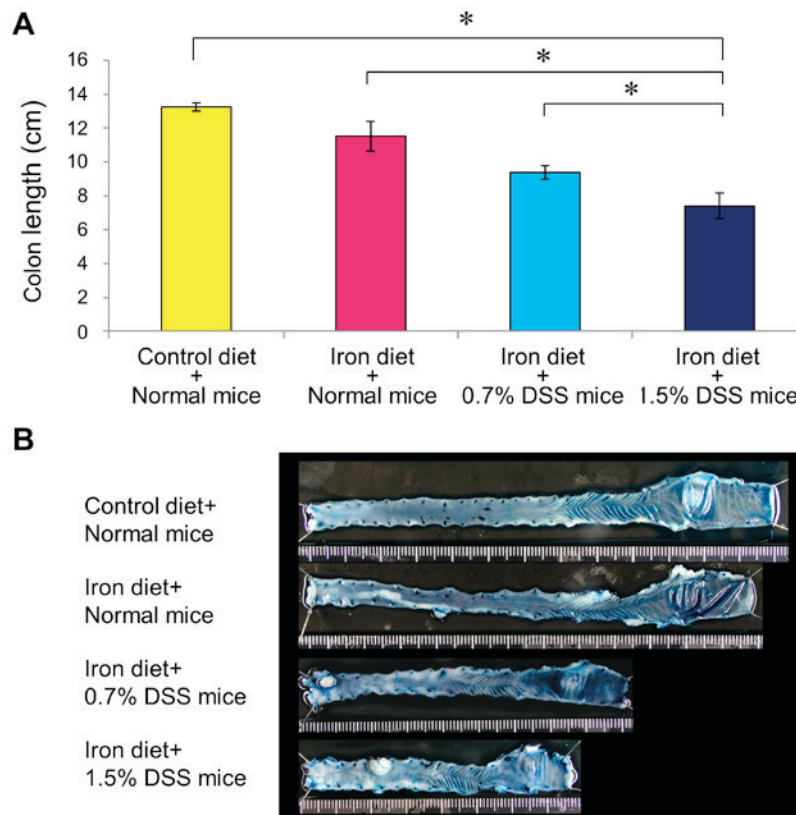


Figure 6. (A) Colon length in chronic DSS-induced colitis. Following 15 cycles of DSS administration, the mice were sacrificed and the severity of colitis was evaluated based on the colonic length from the ceco-colonic junction to the anal verge. (B) Gross appearances of the representative case of DSS groups (following topical application of 0.2% indigo carmine). Colon tumors were observed mostly in the distal part of the colon in the DSS groups. \*P<0.0001. DSS, dextran sulfate sodium. The scale is graduated in millimeters.

Table II. Incidence of colonic tumors induced by chronic DSS exposure.

Experimental group	Negative, n	Indefinite, n	LGD tumor/mouse, n	HGD tumor/mouse, n	LGD+HGD tumor/mouse, n
Control diet + normal mice (n=11)	6	0	0	0	0
Iron diet + normal mice (n=16)	4	1	1/1	0	1/1
Iron diet + 0.7% DSS mice (n=20)	0	13	5/4	4/4	9/7
Iron diet + 1.5% DSS mice (n=10)	0	1	8/5	7/6	15/9

HGD, low-grade dysplasia; LGD, low-grade dysplasia; DSS, dextran sulfate sodium.

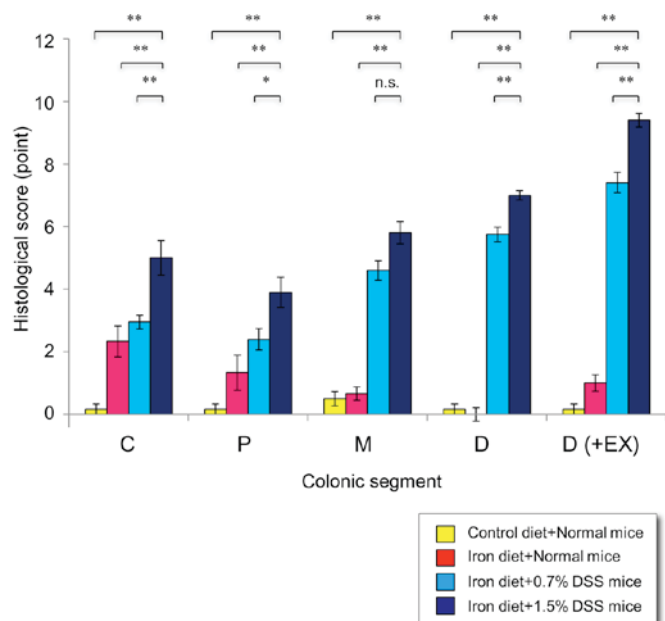


Figure 7. Histological scores in mice with chronic DSS-induced colitis. Following 15 cycles of DSS administration, the mice were sacrificed and the colons were examined histologically. The histologic score for each segment (cecum, proximal colon, middle colon and distal colon) ranged from 0-9 and represented the sum of the scores for the severity of inflammation, damage/necrosis and regeneration. The total histologic score ranged from 0-12 and consisted of the sum of the score for the distal colon and the score for disease extent. \* $P<0.05$  and \*\* $P<0.01$  vs. in the 1.5% DSS mice fed an iron diet. C, cecum; P, proximal colon; M, middle colon; D, distal colon; D (+Ex), distal colon plus disease extent; DSS, dextran sulfate sodium.

diet, suggesting that dietary iron supplementation did not significantly affect tumor development. A total of 9/10 (90.0%) mice treated with 1.5% DSS plus an iron-enriched diet developed dysplasia, with a mean tumor multiplicity of 1.7 tumors per tumor-bearing mouse (15/9). A total of 7/20 mice (35%) treated with 0.7% DSS plus iron-enriched diet developed dysplasia, with a mean tumor multiplicity of 1.3 tumors per tumor-bearing mouse (9/7). The incidences and the multiplicities of dysplasia were significantly higher in the 1.5% DSS mice fed the iron-enriched diet compared with in the 0.7% DSS mice fed the iron-enriched diet. The colonic tumors were confirmed using a histopathological analysis and were classified as indefinite, LGD and HGD. Of the 15 areas of dysplasia in the 1.5% DSS mice fed the iron-enriched diet, HGD was observed in 46.7% (7/15) and LGD was observed in 53.3% (8/15). Of the 9 areas in the 0.7% DSS mice fed the

iron-enriched diet, HGD was observed in 44.4% (4/9) and LGD was observed in 55.6% (5/9).

*Analysis of dysplasia in DSS-induced colitis.* The areas of dysplasia in the DSS mice were further characterized according to pathological and morphological variables. HGD was predominantly located in the distal colon (Fig. 8A). The lesion size was larger for HGD compared with for LGD (Fig. 8B).

Finally, the histopathological diagnosis was compared with the pit pattern assessment. When compared with LGD, HGD exhibited a higher frequency of elevated lesions (Is and IIa) and a lower frequency of flat lesions (IIb) based on the macroscopic features (Fig. 8C); furthermore,  $V_1$  pits were more numerous and IV, III<sub>L</sub> and II pits were less numerous (Fig. 8D). Fig. 9 exemplifies the stereomicroscopic and histological pictures of colonic tumor in a mouse with DSS colitis.

## Discussion

UC patients are well-known to have a higher risk of developing colorectal cancer compared with the general population. The early detection of premalignant and malignant lesions remains the best means of reducing the risk of mortality from colorectal cancer (2,3). The use of animal models allows the design of novel methods to screen for early signs of colon cancer (17,18). These models will expand our understanding of the mechanisms underlying tumor formation and may be useful to identify novel response indicators that are correlated with the early stages of tumorigenesis. Finally, these animal models allow preclinical testing of novel treatment strategies for prevention and intervention.

Long-lasting active inflammation may be an important factor during the earlier stage of the initiation of dysplasia and cancer. A previous study demonstrated that the simple repeated administration of DSS induced dysplasia in mice with a low tumor incidence (20). Subsequently, Seril *et al.* (22) revealed that a 2-fold dietary iron supplementation enhanced the development of DSS-induced dysplasia resulting in a tumor incidence of >70% tumor, partly due to the augmentation of oxidative and nitrosative stress (22,23). Using this modified model, the present study characterized colonic tumors with respect to their morphology and histology.

The present study demonstrated a higher incidence and multiplicity of dysplastic lesions in the 1.5% DSS mice compared with in the 0.7% DSS mice. This finding suggested that the incidence of colitis-induced tumors increased with

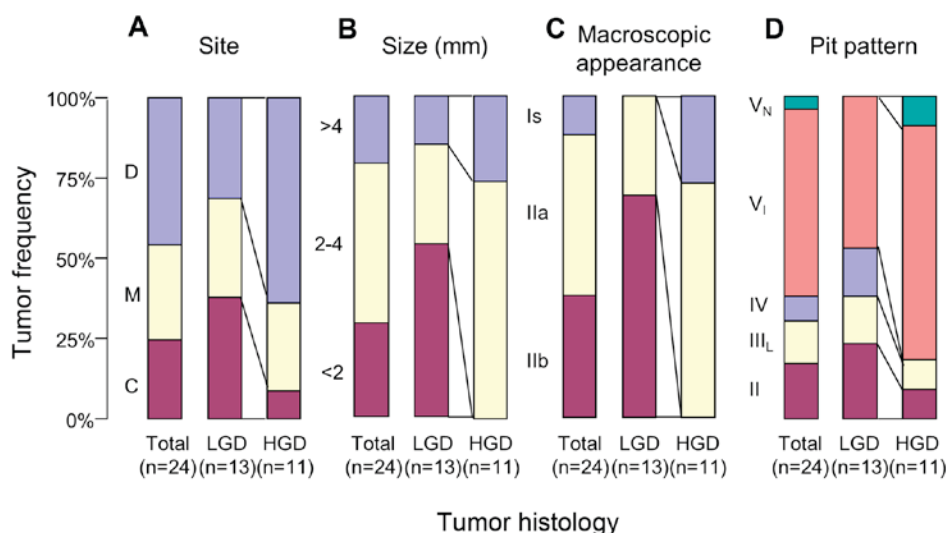


Figure 8. Analysis of colonic tumors induced by chronic dextran sulfate sodium exposure. Colonic tumors were further characterized according to the (A) site, (B) size, (C) macroscopic appearance (D) and pit pattern. LGD, low-grade dysplasia; HGD, high-grade dysplasia; C, cecum; M, middle colon; D, distal colon.

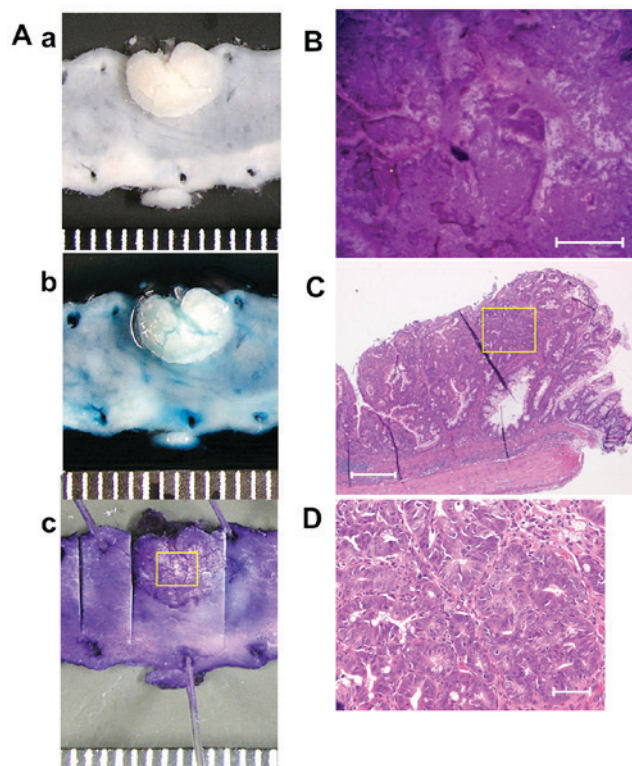


Figure 9. Representative stereomicroscopic and histological images of colonic tumor in a case with chronic dextran sulfate sodium-induced colitis. (A-a) Gross appearances prior to dye-application, (b) following application of 0.2% indigo carmine and (c) following application of 0.06% crystal violet. The scale is graduated in millimeters. (B) Magnified view of the yellow square in (A-c) revealed pit pattern type  $V_N$ . Scale bars, 1 mm. (C) High-grade dysplasia in the elevated lesion was histologically observed. Hematoxylin and eosin stain; original magnification,  $\times 4$ ; scale bar,  $500 \mu\text{m}$ . (D) Magnified view of the yellow square in C. Original magnification,  $\times 40$ ; scale bar,  $50 \mu\text{m}$ .

the severity of inflammation, similar to data for UC in humans (3,34,35).

When compared with LGD, HGD was predominantly located in the distal colon, was larger in size and had a higher incidence of elevated lesions (Is and IIa) and a lower incidence

of flat lesions (IIb), according to its macroscopic features. Although invasive cancer was not observed in the present study, these findings agree with data for UC in humans that revealed that dysplasia and early cancer are predominantly located in the distal colon and exhibit protruded or flat-elevated features (3,34,35). Furthermore, long-term studies using the presently reported DSS colitis model may be useful for studying the sequence of HGD and colitis-associated cancer.

The most important aim of the present study was to investigate whether the pit pattern classification in humans is applicable to the murine model used. The pit pattern classification reported by Kudo *et al* (30,31) divides colonic lesions into 5 classes: Lesions classified as having a I-II pit pattern are generally considered to have benign histology, whereas type III-V pit patterns tend to predict neoplastic lesions (30,31). Previous studies in patients with UC have revealed that the dysplastic lesions and early cancer had type IIIS-IIIL or type IV pits (12). A previous study demonstrated that 13/15 (86.7%) dysplasia/cancer lesions in UC exhibited a neoplastic pit pattern (10), suggesting that a pit pattern analysis may be useful for detecting and discriminating neoplastic lesions in UC, although coexisting inflammatory changes may modify the mucosal details.

The present study used stereomicroscopy with dye-application to improve the detection of epithelial changes representing neoplastic or dysplastic alterations. To the best of our knowledge, using the pit pattern classification, the present study demonstrated for the first time that HGD exhibited an increased incidence of type  $V_I$  pits and a decreased incidence of type IV, III<sub>L</sub> and II pits. This allowed the present study to classify the colonic tumors with regards to their pit pattern even in colitis-induced tumors in mice. Therefore, consistent with studies examining UC in humans (10-16), chromoendoscopy has emerged as a useful approach for detecting and discriminating neoplastic changes in colitis-associated tumors in mice.

Previously, a safe method for performing endoscopy in mice was developed, permitting long-term studies in living mice (36). Using this method, further study may aid investigators to determine the success of their experiment *in vivo* at an

early stage and to reduce the number of animals required for experiments examining prevention or interventions.

In conclusion, the repeated administration of DSS with iron-supplementation induced dysplastic lesions with a high incidence. Pit pattern evaluations using stereomicroscopy with dye-application were useful for detecting and discriminating neoplastic changes in DSS mice and may be useful for furthering our understanding of the mechanisms underlying tumor formation in UC patients and the characterization of pharmaceutical responses.

### Acknowledgements

The present study was supported in part by a Grant-in-Aid from the Japanese Ministry of Education, Culture and Science (grant no. 25460964) and the Health and Labour Sciences Research Grants for research on intractable diseases from the Ministry of Health, Labour and Welfare of Japan.

### References

1. Strober W, Fuss I and Mannon P: The fundamental basis of inflammatory bowel disease. *J Clin Invest* 117: 514-521, 2007.
2. Eaden JA, Abrams KR and Mayberry JF: The risk of colorectal cancer in ulcerative colitis: A meta-analysis. *Gut* 48: 526-535, 2001.
3. Ullman TA and Itzkowitz SH: Intestinal inflammation and cancer. *Gastroenterology* 140: 1807-1816, 2011.
4. Morson BC and Pang LS: Rectal biopsy as an aid to cancer control in ulcerative colitis. *Gut* 8: 423-434, 1967.
5. Bernstein CN, Shanahan F and Weinstein WM: Are we telling patients the truth about surveillance colonoscopy in ulcerative colitis? *Lancet* 343: 71-74, 1994.
6. Blackstone MO, Riddell RH, Rogers BH and Levin B: Dysplasia-associated lesion or mass (DALM) detected by colonoscopy in long-standing ulcerative colitis: An indication for colectomy. *Gastroenterology* 80: 366-374, 1981.
7. Basu S, Torigian D and Alavi A: The role of modern molecular imaging techniques in gastroenterology. *Gastroenterology* 135: 1055-1061, 2008.
8. Axelrad AM, Fleischer DE, Geller AJ, Nguyen CC, Lewis JH, Al-Kawas FH, Avigan MI, Montgomery EA and Benjamin SB: High-resolution chromoendoscopy for the diagnosis of diminutive colon polyps: Implications for colon cancer screening. *Gastroenterology* 110: 1253-1258, 1996.
9. Fu KI, Sano Y, Kato S, Fujii T, Nagashima F, Yoshino T, Okuno T, Yoshida S and Fujimori T: Chromoendoscopy using indigo carmine dye spraying with magnifying observation is the most reliable method for differential diagnosis between non-neoplastic and neoplastic colorectal lesions: A prospective study. *Endoscopy* 36: 1089-1093, 2004.
10. Yoshioka S, Mitsuyama K, Takedatsu H, Kuwaki K, Yamauchi R, Yamasaki H, Fukunaga S, Akiba J, Kinugasa T, Akagi Y, *et al*: Advanced endoscopic features of ulcerative colitis-associated neoplasias: Quantification of autofluorescence imaging. *Int J Oncol* 48: 551-558, 2016.
11. Watanabe T, Ajioka Y, Mitsuyama K, Watanabe K, Hanai H, Nakase H, Kunisaki R, Matsuda K, Iwakiri R, Hida N, *et al*: Comparison of targeted vs random biopsies for surveillance of ulcerative colitis-associated colorectal cancer. *Gastroenterology* 151: 1122-1130, 2016.
12. Sada M, Igarashi M, Yoshizawa S, Kobayashi K, Katsumata T, Saigenji K, Otani Y, Okayasu I and Mitomi H: Dye spraying and magnifying endoscopy for dysplasia and cancer surveillance in ulcerative colitis. *Dis Colon Rectum* 47: 1816-1823, 2004.
13. Hata K, Watanabe T, Kazama S, Suzuki K, Shinozaki M, Yokoyama T, Matsuda K, Muto T and Nagawa H: Earlier surveillance colonoscopy programme improves survival in patients with ulcerative colitis associated colorectal cancer: Results of a 23-year surveillance programme in the Japanese population. *Br J Cancer* 89: 1232-1236, 2003.
14. Matsumoto T, Nakamura S, Jo Y, Yao T and Iida M: Chromoscopy might improve diagnostic accuracy in cancer surveillance for ulcerative colitis. *Am J Gastroenterol* 98: 1827-1833, 2003.
15. Kiesslich R, Goetz M, Lammersdorf K, Schneider C, Burg J, Stolte M, Vieth M, Nafe B, Galle PR and Neurath MF: Chromoscopy-guided endomicroscopy increases the diagnostic yield of intraepithelial neoplasia in ulcerative colitis. *Gastroenterology* 132: 874-882, 2007.
16. Kiesslich R, Fritsch J, Holtmann M, Koehler HH, Stolte M, Kanzler S, Nafe B, Jung M, Galle PR and Neurath MF: Methylene blue-aided chromoendoscopy for the detection of intraepithelial neoplasia and colon cancer in ulcerative colitis. *Gastroenterology* 124: 880-888, 2003.
17. Kiesler P, Fuss IJ and Strober W: Experimental models of inflammatory bowel diseases. *Cell Mol Gastroenterol Hepatol* 1: 154-170, 2015.
18. Kanneganti M, Mino Kenudson M and Mizoguchi E: Animal models of colitis-associated carcinogenesis. *J Biomed Biotechnol* 2011: 342637, 2011.
19. Okayasu I, Hatakeyama S, Yamada M, Ohkusa T, Inagaki Y and Nakaya R: A novel method in the induction of reliable experimental acute and chronic ulcerative colitis in mice. *Gastroenterology* 98: 694-702, 1990.
20. Okayasu I, Yamada M, Mikami T, Yoshida T, Kanno J and Ohkusa T: Dysplasia and carcinoma development in a repeated dextran sulfate sodium-induced colitis model. *J Gastroenterol Hepatol* 17: 1078-1083, 2002.
21. Committee for the Update of the Guide for the Care and Use of Laboratory A and National Research Council: Guide for the Care and Use of Laboratory Animals. 8th edition. National Academies Press, Washington, DC, 2011.
22. Seril DN, Liao J, Yang CS and Yang GY: Systemic iron supplementation replenishes iron stores without enhancing colon carcinogenesis in murine models of ulcerative colitis: Comparison with iron-enriched diet. *Dig Dis Sci* 50: 696-707, 2005.
23. Liao J, Seril DN, Yang AL, Lu GG and Yang GY: Inhibition of chronic ulcerative colitis associated adenocarcinoma development in mice by inositol compounds. *Carcinogenesis* 28: 446-454, 2007.
24. Tardif SD, Coleman K, Hobbs TR and Lutz C: IACUC review of nonhuman primate research. *ILAR J* 54: 234-245, 2013.
25. Cooper HS, Murthy SN, Shah RS and Sedergran DJ: Clinicopathologic study of dextran sulfate sodium experimental murine colitis. *Lab Invest* 69: 238-249, 1993.
26. Takaki K, Mitsuyama K, Tsuruta O, Toyonaga A and Sata M: Attenuation of experimental colonic injury by thiazolidinedione agents. *Inflamm Res* 55: 10-15, 2006.
27. Dieleman LA, Ridwan BU, Tennyson GS, Beagley KW, Bucy RP and Elson CO: Dextran sulfate sodium-induced colitis occurs in severe combined immunodeficient mice. *Gastroenterology* 107: 1643-1652, 1994.
28. The Paris endoscopic classification of superficial neoplastic lesions: Esophagus, stomach, and colon: November 30 to December 1, 2002. *Gastrointest Endosc* 58 (6 Suppl): 3-43, 2003.
29. Hata K, Watanabe T, Shinozaki M, Kojima T and Nagawa H: To dye or not to dye? That is beyond question! Optimising surveillance colonoscopy is indispensable for detecting dysplasia in ulcerative colitis. *Gut* 53: 1722, 2004.
30. Kudo S, Hirota S, Nakajima T, Hosobe S, Kusaka H, Kobayashi T, Himori M and Yagyu A: Colorectal tumours and pit pattern. *J Clin Pathol* 47: 880-885, 1994.
31. Kudo S, Tamura S, Nakajima T, Yamano H, Kusaka H and Watanabe H: Diagnosis of colorectal tumorous lesions by magnifying endoscopy. *Gastrointest Endosc* 44: 8-14, 1996.
32. Riddell RH, Goldman H, Ransohoff DF, Appelman HD, Fenoglio CM, Haggitt RC, Ahren C, Correa P, Hamilton SR, Morson BC, *et al*: Dysplasia in inflammatory bowel disease: Standardized classification with provisional clinical applications. *Hum Pathol* 14: 931-968, 1983.
33. Schlemper RJ, Riddell RH, Kato Y, Borchard F, Cooper HS, Dawsey SM, Dixon MF, Fenoglio-Preiser CM, Fléjou JF, Geboes K, *et al*: The Vienna classification of gastrointestinal epithelial neoplasia. *Gut* 47: 251-255, 2000.
34. Barral M, Dohan A, Allez M, Boudiaf M, Camus M, Laurent V, Hoefel C and Soyer P: Gastrointestinal cancers in inflammatory bowel disease: An update with emphasis on imaging findings. *Crit Rev Oncol Hematol* 97: 30-46, 2016.
35. Matkowskyj KA, Chen ZE, Rao MS and Yang GY: Dysplastic lesions in inflammatory bowel disease: Molecular pathogenesis to morphology. *Arch Pathol Lab Med* 137: 338-350, 2013.
36. Becker C, Fantini MC, Wirtz S, Nikolaev A, Kiesslich R, Lehr HA, Galle PR and Neurath MF: In vivo imaging of colitis and colon cancer development in mice using high resolution chromoendoscopy. *Gut* 54: 950-954, 2005.